Three-Dimensional Supersonic Jet Behavior in BOF Multijet Lance with Modified Tip Geometry

Ayrton Cavallini Zotelle[1,2], Pedro Francelino Garcia[2], Renato do Nascimento Siqueira[2], João Paulo Barbosa[2], José Roberto de Oliveira[3] and Breno Totti Maia[4]

[1]GPEMAR, Department of Mechanical Engineering, Federal Center of Technology Celso Suckow da Fonseca – CEFET-RJ campus Angra dos Reis
Areal Street, 522, Parque Mambucaba, Angra dos Reis, RJ, 23.953-030, Brazil
Phone: +55 (24) 3364-1754
E-mail: ayrton.zotelle@cefet-rj.br

[2]LPMF, Department of Mechanical Engineering, Federal Institute of Espírito Santo – IFES campus São Mateus
Rod. BR 101 north, km 58, Litorâneo, São Mateus, ES, 29.932-540, Brazil
Phone: +55 (27) 3767-7010
E-mail: pedrofrancelino@gmail.com; renatons@ifes.edu.br; jpbarbosa@ifes.edu.br

[3]Department of Metallurgical Engineering, Federal Institute of Espírito Santo – IFES campus Vitória
Av. Vitória, 1729, Jucutuquara, Vitória - ES, 29.040-80, Brazil
Phone: +55 (27) 3331-2178
E-mail: jroberto@ifes.edu.br

[4]Lumar Metals – South America
Rod. MG 232 – Km 09,70, Santana do Paraíso – MG, 35.1789-000, Brazil
Phone: +55 (31) 3828-1000
E-mail: breno.totti@lumarmetals.com.br

ABSTRACT

The supersonic multi-jet lance plays a critical role in the operation of Basic Oxygen Furnace (BOF) converters. However, the harsh environment within the converter and the complex fluid dynamic interactions near the lance can significantly reduce its operational lifespan. Proper lance design can alter flow patterns, minimize wear, and extend its service life. Additionally, optimized lance geometry enhances jet quality and oxygen mixing with the molten metal, thereby improving process efficiency and steel quality. This study employs a three-dimensional computational model to analyze the fluid dynamic behavior in BOF converters and assess the influence of lance geometry on flow patterns and metal accumulation at the lance tip – a phenomenon known to impair process performance. Two geometries were investigated: a conventional design based on a typical 300-ton converter and a modified version with a flat face, resulting in an elliptical nozzle outlet. Results indicate that the geometric modification affects jet coalescence and can increase the length of the supersonic core by up to 4.6%, depending on the Nozzle Pressure Ratio (NPR). Furthermore, the altered tip geometry influences the inter-jet flow patterns, which may help reduce metal buildup at the lance tip and ultimately extend its lifespan.

Keywords: Basic Oxygen Furnace, supersonic multi-jet lance, nozzle pressure ratio, lance tip geometry, jet coalescence, flow pattern optimization, lance wear reduction

INTRODUCTION

The supersonic multi-jet lance is a key component in Basic Oxygen Furnace (BOF) steelmaking converters, responsible for delivering oxygen at high velocities to promote efficient chemical reactions in the molten metal bath[1-4]. The conversion of oxygen pressure energy into kinetic energy through multiple supersonic jets enhances mixing and reaction rates, which are essential for the effective refining of steel[5]. However, the harsh and aggressive environment inside BOF converters, combined with the complex fluid dynamic interactions near the lance tip, impose significant challenges to its operational durability.

Early investigations centered on single nozzles clarified fundamental features of supersonic jets, but ignored the inter-jet coupling characteristic of industrial lances[2]. In multi-nozzle configurations, entrainment of the surrounding gas lowers the static pressure between adjacent jets; the resulting pressure gradients induce mutual deflection and eventual coalescence, as quantified by Wang et al.[6].

Among the various factors influencing jet coalescence and overall BOF performance, the number of nozzles is particularly significant. Configurations employing three to six nozzles are commonly reported in the literature[2-3,7-9]. The primary goal of using multiple nozzles is to increase the oxygen flow rate, while minimizing slopping and reducing premature damage to the refractory lining. Sambasivam et al.[10] also proposed a seven-nozzle design, incorporating a central subsonic jet. Their combined computational and experimental analysis revealed that the central jet does not induce coalescence, and it significantly enhances droplet generation compared to traditional six-nozzle configurations. Furthermore, this design prolongs the lance tip's operational life by reducing wear.

In addition to the number of nozzles, their orientation in relation to the lance axis (inclination and twist angle) also affect jet behavior and converter performance. Wang et al.[6] numerically investigated the impact of inclination angle on jet interaction, concluding that smaller inclination angles result in stronger interference and increased coalescence. Higuchi and Tago[11] studied six-nozzle lances with twisted configurations, where the nozzle and lance axes do not intersect, and concluded that, in their cold-model experiments, a twist angle of 11.4º minimizes spitting. Maia et al.[8] extended this investigation to four-nozzle lances, showing that while a 10º twist still resulted in coalescence, a 20º twist promoted independent jets and improved atomization at the bath surface.

The internal geometry of the nozzles also plays a crucial role on the process performance. While trapezoidal CD nozzles are standard, alternative geometries such as curvilinear, truncated, and compressed profiles have been proposed. Garcia et al.[4] compared these designs, showing that truncated nozzles intensify oblique shocks from the exit, whereas compressed nozzles amplify shocks from the throat region. The curvilinear geometry demonstrated superior performance, with higher Mach numbers and extended potential core lengths compared to the trapezoidal design, indicating enhanced capacity for turbulence generation at greater distances within the molten bath.

BOF performance is influenced not only by geometric factors but also by operational parameters. In practice, the operating pressure often deviates from design values due to equipment and process fluctuations. To avoid undesirable overexpanded flow regimes, which can lead to increased lance wear, and to ensure sufficient impact force at the bath surface, higher operating pressures are typically employed. These ensure that the nozzle exit pressure remains above the ambient pressure, resulting in a favorable nozzle pressure ratio (NPR). Higher NPR values not only prevent wear but also extend the supersonic and potential core lengths of the jets, thereby improving mixing efficiency[2].

Besides all the advances in BOF lance design, wear at the lance tip is still a major concern in industrial steelmaking[12]. The high-temperature environment, slag, and molten metal droplets can adhere to the cooled lance surface, especially in the central region between jets, disrupting jet flow and accelerating wear. Such metal buildup not only reduces the lance's service life but can also negatively impact process efficiency and steel quality. Thus, a proper design of the lance tip is a critical factor that influence flow patterns, jet quality, and ultimately the lance's operational performance.

The present study therefore evaluates a modified flat-faced tip that transforms each circular outlet into an elliptical one. A validated three-dimensional CFD model is employed to compare the conventional and modified geometries across representative NPR values. The analysis quantifies variations in jet coalescence, supersonic-core length, and inter-jet recirculation, thereby providing a mechanistic basis for assessing the modified tip's potential to mitigate metal accretion in the lance tip, and extend its operational lifespan.

MATHEMATICAL FORMULATION

The evaluation of the geometry effects on the supersonic structures is a three-dimensional, compressible, turbulent, and steady problem. It can be solved using a Reynolds Averaged Navier-Stokes (RANS) model to obtain the mean velocity and pressure fields with the effects of turbulent fluctuations being modeled by the Boussinesq hypothesis, to reduce the computational cost. The continuity equation is given by:

$$\nabla \cdot (\rho \boldsymbol{u}) = 0\,, \tag{1}$$

where $\boldsymbol{u}$ is the mean velocity vector and ρ is the density of the fluid that, for an ideal gas, can be expressed by:

$$\rho = \rho_0 \left(1 + \frac{K-1}{2} Ma^2\right)^{\frac{1}{1-K}}, \tag{2}$$

in which ρ_0 is the air density at the reference temperature (300 K), $K = 1.4$ is the ratio of specific heat of the air at constant pressure (C_p) to its specific heat at constant volume (C_v), and $Ma = |\boldsymbol{u}|/c$ is the Mach number. The sound velocity is calculated for each cell of the computational domain as $c = \sqrt{KRT}$. $R = \bar{R}/M$ is the specific gas constant for the air, $\bar{R} = 8.314\ kJ/(kmol\ K)$ is the universal gas constant, M is the air molecular weight and T is the air temperature. The momentum equation is:

$$\nabla \cdot (\rho \boldsymbol{u}\boldsymbol{u}) = -\nabla P + \nabla \cdot \left[(\mu + \mu_t)\left(\nabla \boldsymbol{u} + \nabla \boldsymbol{u}^T - \frac{2}{3}\nabla \cdot \boldsymbol{u}\, \boldsymbol{I}\right) - \frac{2}{3}k\boldsymbol{I}\right], \tag{3}$$

where P is the pressure field, μ and μ_t are the molecular and turbulent viscosity, respectively, and $k = \left(\overline{\boldsymbol{u}' \cdot \boldsymbol{u}'}\right)/2$ is the turbulent kinetic energy. The temperature field is determined by solving the energy equation (Eq. 4) throughout the numerical domain:

$$\nabla \cdot [\boldsymbol{u}(\rho E + P)] = \nabla \cdot \left[(\lambda + \lambda_T)\nabla T + \mu\left(\nabla \boldsymbol{u} + \nabla \boldsymbol{u}^T - \frac{2}{3}\nabla \cdot \boldsymbol{u}\, \boldsymbol{I}\right) \cdot \boldsymbol{u}\right], \tag{4}$$

in which $E = C_p T - P/\rho + |\boldsymbol{u}|^2/2$, and λ and λ_T are the molecular and turbulent thermal conductivities, respectively.

The turbulent viscosity μ_t and the turbulent thermal conductivity λ_T were obtained by the application of a turbulence closure model (Eq. 5 and Eq. 6). The *k-ω* SST (Shear Stress Transport) model is widely used in the literature to simulate supersonic flows in Laval nozzles[4,13,14] and was also used in this work. The *k-ω* SST model was developed by Mender[15] and has hybrid characteristics that make it suitable for simulations with adverse pressure gradients and the presence of walls, using the robust and accurate *k-ω* model in the region close to the wall and the *k-ε* model in the regions of potential flow[16]. In this model, the turbulent viscosity is given by $\mu_t = \rho\sigma_t k/\omega$, where σ_t is a model constant, and the thermal conductivity by $\lambda_T = \lambda\mu_t/\mu$. The turbulence model equations are the turbulent kinetic energy (k) equation:

$$\nabla \cdot (\rho \boldsymbol{u} k) = \nabla \cdot \left[\left(\mu + \frac{\mu_t}{\sigma_k}\right)\nabla k\right] + G_k - Y_k\,, \tag{5}$$

and the specific dissipation rate (ω) equation:

$$\nabla \cdot (\rho \boldsymbol{u} \omega) = \nabla \cdot \left[\left(\mu + \frac{\mu_t}{\sigma_\omega}\right)\nabla \omega\right] + G_\omega - Y_\omega + D_\omega\,, \tag{6}$$

For these equations, σ_k and σ_ω are empirical constants. G_k is the production of turbulence kinetic energy, G_ω is the generation of ω, Y_k and Y_ω are the dissipation of k and ω due to turbulence and D_ω represents the cross-diffusion term. The constants used (σ_t, σ_k, and σ_ω) were the default values of ANSYS Fluent[16].

An essential description for compressible flows is how compressibility affects the dissipation rate of k and ω. A compressibility function, $F(M_t)$, is used to insert the compressibility effects on the k-ω SST model, so that the dissipation of k becomes:

$$Y_k = \tilde{Y}_k[1 + \zeta^* F(M_t)]\,, \tag{7}$$

and the dissipation of ω:

$$Y_\omega = \tilde{Y}_\omega\left[1 + \frac{\beta_i^*}{\beta_i}\zeta^* F(M_t)\right], \tag{8}$$

where Y_k and Y_ω are the dissipation of k and ω for the incompressible case. The constants ζ^* and β_i and the function β_i^* are default of ANSYS Fluent[16]. The compressibility function is:

$$F(M_t) = \begin{cases} 0, & if\ \dfrac{\sqrt{2k}}{c} \leq 0.25 \\ \dfrac{2k}{c^2} - \dfrac{1}{16}, & if\ \dfrac{\sqrt{2k}}{c} > 0.25 \end{cases}. \tag{9}$$

It is observed that for low values of turbulent kinetic energy, the compressibility effects are negligible, and the rate of dissipation becomes $Y_k = \tilde{Y}_k$ and $Y_\omega = \tilde{Y}_\omega$.

NUMERICAL METHOD

The geometry of the oxygen lance is based on the real geometry of typical converters of 300t steel production capacity[17]. The lance has 6 nozzles, with an axial symmetry configuration. Some geometric simplifications were proposed to simplify the analyses, such as a flat face on the front of the lance and a perpendicular flat face for each nozzle. The details of the lance geometry are shown in Fig. 1. To evaluate the influence of the geometry of the nozzle, a continuity of the divergent section was proposed, as shown on the right side of the figure. This modification turns the outlet section of the lance into an elliptical form.

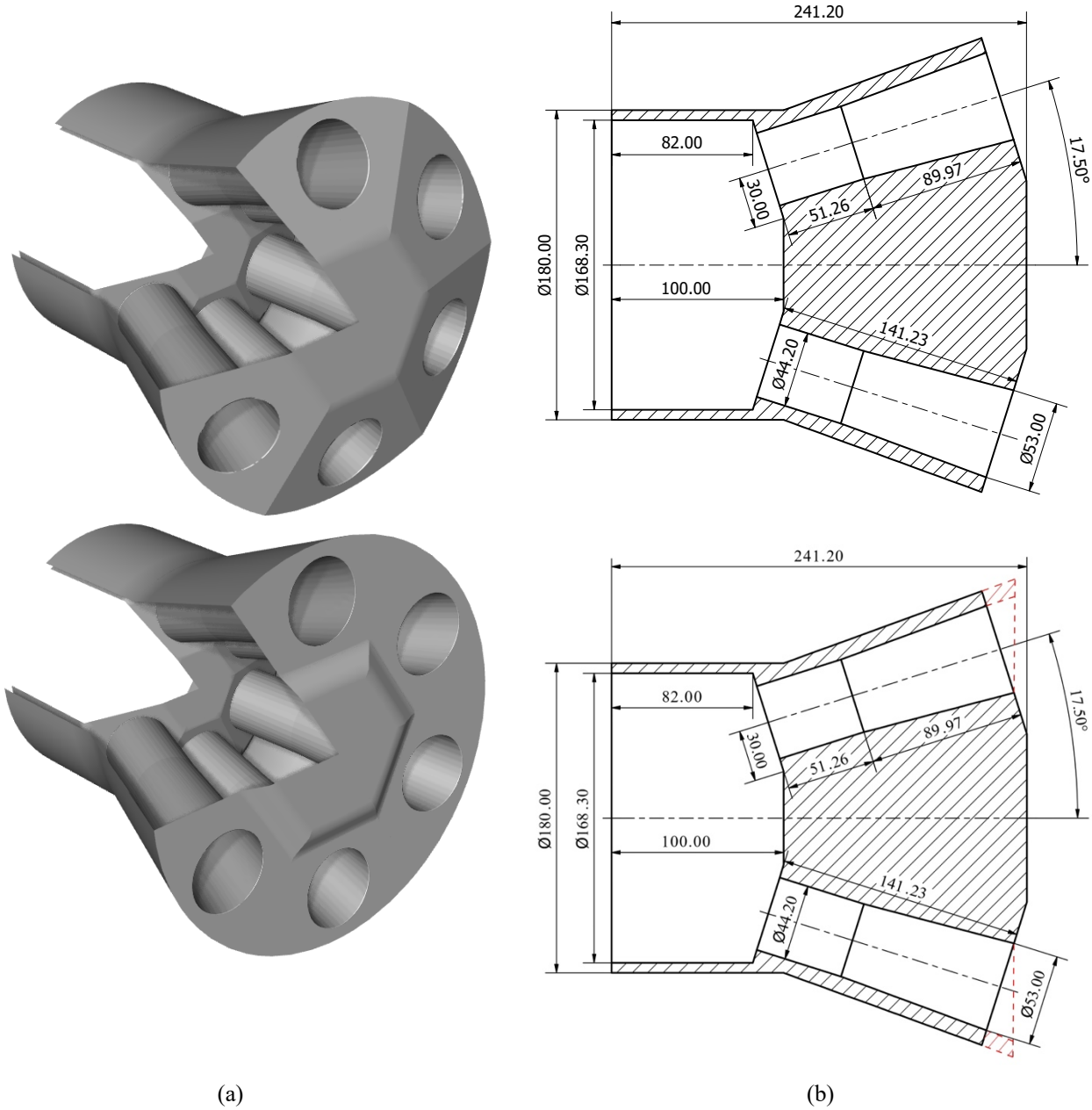

(a) (b)

Figure 1. Geometry of BOF lance used in the simulations (a) isometric view of the original and modified lance and (b) sectional view with dimensional description of lance and nozzle.

Due to the complexity of the flow, most of the supersonic jet simulations are performed in the two-dimensional plane or using axisymmetric conditions due to the large amount of computational time required for three-dimensional simulations[4,18,19]. As reported by Raje and Sinha[20], the multi-jet interaction is quite complex and involves the occurrence of various flow structures, flow regimes, and large thermal and momentum gradients. Such flows span from subsonic to supersonic Mach numbers and consist of a multitude of shocks and expansion waves. There are regions of strong inviscid/viscous interactions involving free shear layers, boundary layers, shocks, separated flow and recirculation regions, and plume/plume interaction. Additionally, the flow field induced by multiple jets can be highly three-dimensional. The complex multi-nozzle configuration and the structural base requires elaborate grid generation and thus CFD simulation of these flows is an exceptionally challenging task. However, three-dimensional Unsteady Reynolds-averaged Navier-Stokes (URANS) simulations remain a viable option to predict the multi-jet interaction flow field and the associated base pressure and base heat flux. To simulate the three-dimensional problem, some artifices were used. The domain consists of a 60º slice of the full geometry, representing a unique nozzle. The external domain was constructed with 10,000 mm length and 2,000 mm radius.

For the boundary conditions, the walls of the lance and nozzle had no slip condition. The two lateral boundary conditions (yellow on Fig. 2) were periodic. It means that the tangential component of the velocity has no gradient on the face, and the normal component of velocity is associated with the velocity on the other correspondent periodic face, i.e., the outer flux on one face is equal to the inner flux in the periodic correspondent face. The external face of the cylinder is treated as free slip, the gradient of the tangential component of the velocity is null, and the normal component is zero. The fluid inlet boundary condition consists of 300 K temperature and absolute pressure determined by the nozzle pressure ratio (NPR) value:

$$NPR = \frac{P_{in}}{P_0}, \tag{10}$$

in which P_{in} is the inlet absolute pressure and P_0 the surrounding pressure. The outlet boundary condition has an absolute pressure of 1 atm and 300 K temperature. An overview of the geometry dimensions and boundary conditions that were used in this work is shown in Fig. 2, except for the nozzle, which is given in Fig. 1.

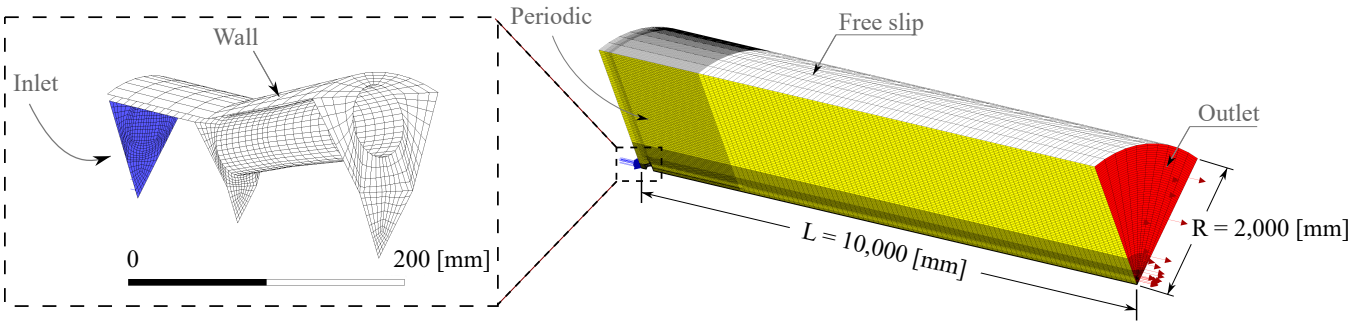

Figure 2. Numerical geometry and boundary conditions.

For mesh generation, homogeneous hexahedra elements were used. This type of mesh was chosen due to its orthogonal quality near to one. A coarse basic mesh was constructed, and an adaptive mesh method was used to refine the mesh in the regions where the supersonic structures are present, i.e., high density gradients and high Mach numbers. The cut-cell method consists of dividing the original mesh into levels of refinement. For a three-dimensional simulation, each cell is divided into $N = 2^{3n}$ elements, in which n represents the maximum level of refinement, as illustrated in Fig. 3.

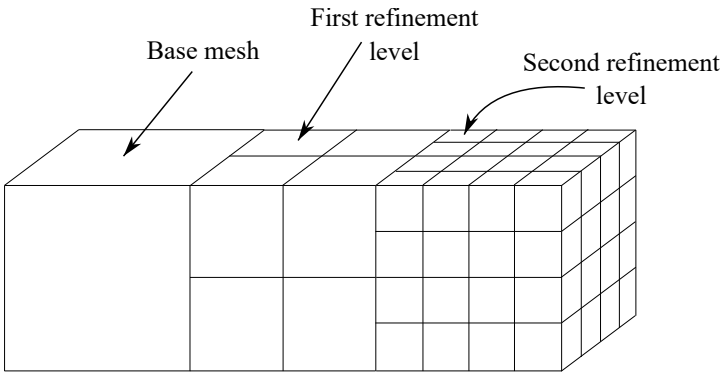

Figure 3. Example of the automatic mesh adaptation using three-dimensional cut-cell method.

Two refinement criteria were used: for the description of the supersonic core, cells with Mach number in the range $0.8 \leq Ma \leq 1.20$ were refined; and for the representation of the potential core and shock waves, regions with density ratios equal or higher than 0.5 times the global mean density gradient for the whole domain were refined. The maximum refinement level was determinate based on the mesh independence test.

The numerical methods used to perform the simulations were all implicit-based schemes, including COUPLED algorithms for pressure-velocity coupling. For spatial discretization, third-order methods were used for density and momentum, and all the other methods were second order. The simulations were performed using the commercial CFD software Ansys FLUENT©. An overview of the fluid properties and solution methods are listed on Tab. 1.

Table 1: Fluid properties and numerical methods applied to simulations.

Material (dry air)	Density at ambient temperature (ρ_0)		$1.225\ kg/m^3$
	Specific hear at constant pressure (C_p)		$1006.43\ J/kg\ K$
	Molecular viscosity (μ)		$1.7897\ x10^{-05}\ Pa\ s$
	Molecular weight (M)		$28.966\ kg/kmol$
	Thermal conductivity (λ)		$0.0242\ W/mK$
Surrounding condition	Ambient temperature (T_0)		$300\ K$
	Ambient pressure (P_0)		1 atm
Solution methods	Pressure-velocity coupling		Coupled
	Spatial discretization	Gradient	Least Squares Cell Based
		Pressure	Second order
		Momentum	Third-order MUSCL
		Density	Third-order MUSCL
		Energy	Second order Upwind
		Turbulent kinetic energy	Second order Upwind
		Specific dissipation rate	Second order Upwind

RESULTS AND DISCUSSIONS

The first step of this work was the evaluation of the capability of the model to represent the physical phenomenon, i.e., the supersonic structures of a three-dimensional flow in a convergent-divergent nozzle. The experimental results of Zapryagaev[21] were used as reference. Schlieren pictures (density gradients) were simulated for two values of NPR and a comparison of the simulations with the experimental results were used to validate the model (Fig. 1).

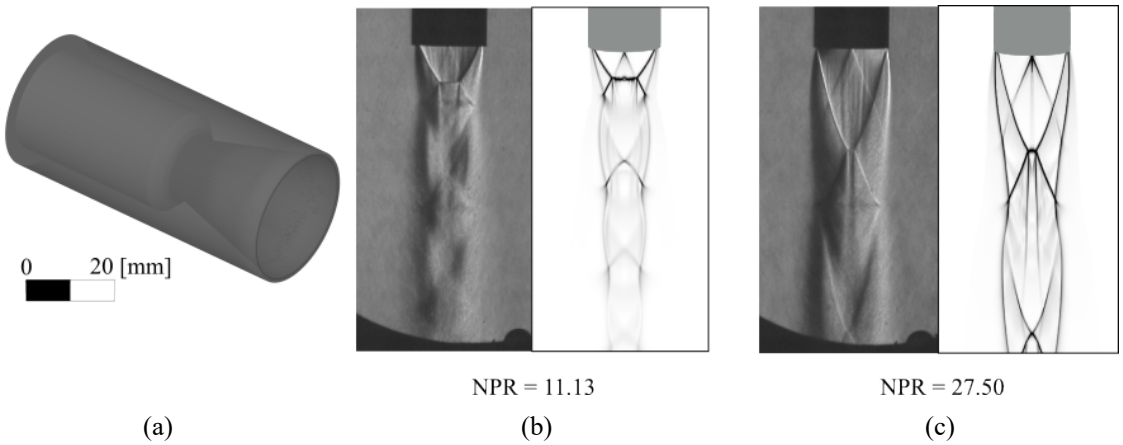

Figure 4. Comparison between the Schilieren images obtained experimentally by Zapryagaev et al.[21] (left) and with the three-dimensional numerical simulations (right).

The nozzle used by Zapryagaev[21], which was simulated to validate the model, is shown in Fig. 4(a) on left, and the results for the NPR values of 11.13 and 27.50 are shown in Fig. 4(b) and Fig. 4(c), respectively. On these figures, the left Schlieren pictures refer to the experimental work of Zapryagaev[21], and the right pictures refer to the simulations (this work). The simulation images were slightly tilted to obtain a visualization angle like the used by the camera to take the pictures in the experimental setup. The main patterns of the flow were well represented by the model, like the strong normal shock close to the nozzle outlet for NPR = 11.13 and the slip region in the central part for NPR = 27.50. It is noticed that the numerical model was capable of correctly predicting the flow behavior, validating the model to perform the simulations proposed in this work.

The next step after the model validation was to perform the grid independence test. The images shown in Fig. 5 are composed of two parts. The left side of the image refers to the Schlieren pictures obtained at the simulations, while the right side refers to the respective mesh. The results were plotted on the *rz*-plane, passing through the middle of the nozzle. The simulations were performed for NPR = 12 and 5 refinement levels (n = 0; 1; 2; 3 and 4). It is possible to observe in Fig. 5 that some flow characteristics were not captured by the initial mesh (n = 0) and the first refinement level (n = 1). For n = 2, the main characteristics are observed, but some details inside the nozzle and close to the nozzle outlet are not so clear. For the refinement levels n = 3 and n = 4, no significant changes of the potential core are observed, while the number of elements increases from 5,520,393 to 28,524,339, significantly increasing the computational cost and, therefore, the time of the simulation. For this reason, level n = 3 was considered appropriate for the simulations.

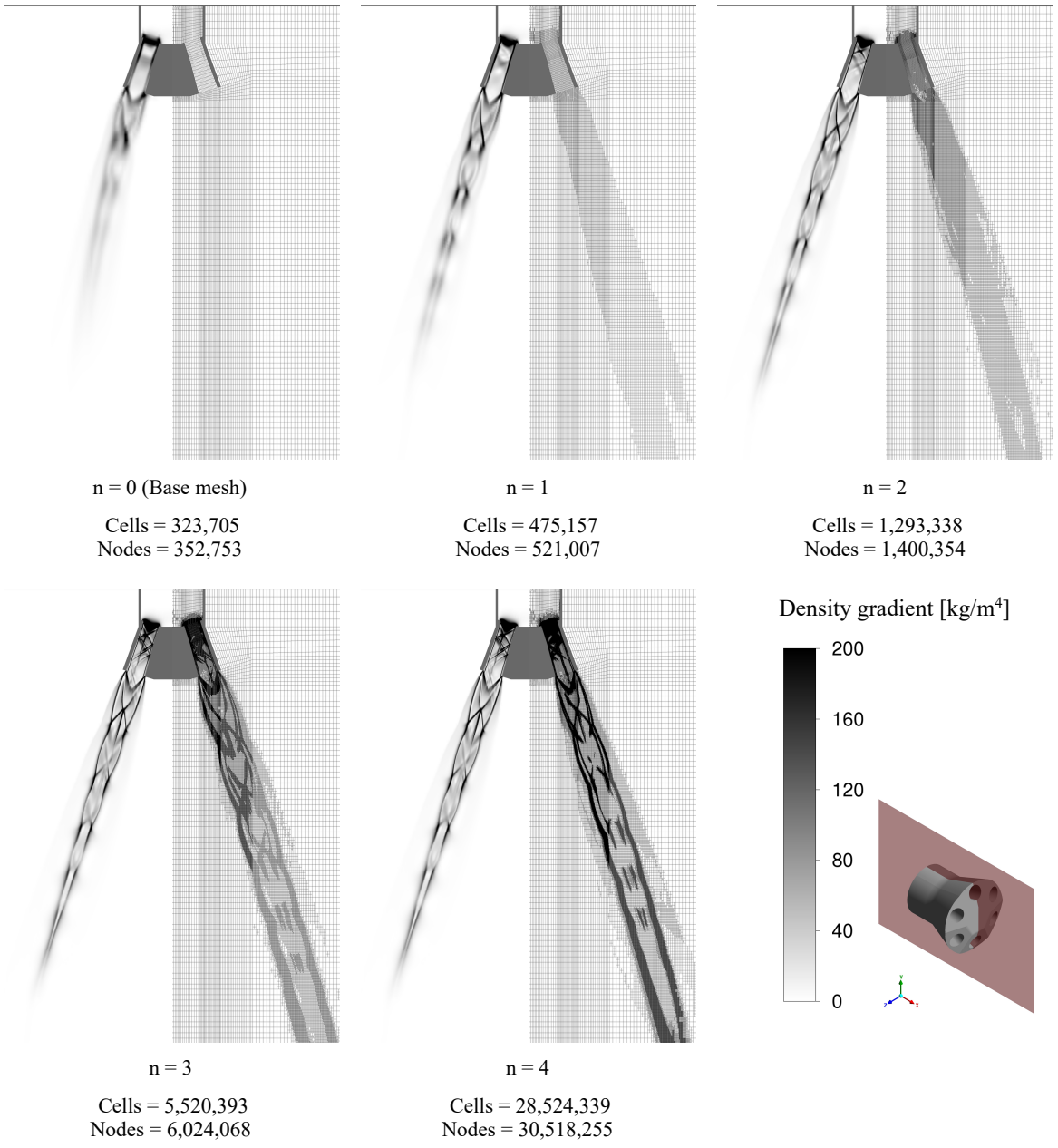

Figure 5. Influence of mesh refinement on Schilieren images and shock indicators.

After validating the model and choosing the appropriate mesh for the case of this study, the analysis of flow patterns and their consequences on BOF process can be carried out. Figure 6 shows the Mach number contours for the original and modified configuration at different NPR values. The original configuration results are depicted in the first column, while the modified configuration results are shown in the second column. In the top row, are the results for the NPR = 4 case. As expected, for this pressure ratio, the flow is overexpanded, and Mach disks and subsonic areas are seen in the core of the jet. The flow patterns for both configurations are quite similar, but in the original geometry case (left side of first row), the subsonic regions within the jet are more centered and slightly larger. For the modified configuration case (right side of first row), the subsonic regions are smaller and asymmetric in relation to the jet center line. The asymmetry of the supersonic jet observed for the modified configuration at NPR = 4 is the reason for the smaller coalescence of the jet in this case, since momentum is transferred to the outer region of the jet. For the other NPR cases that were analyzed, this behavior was not observed.

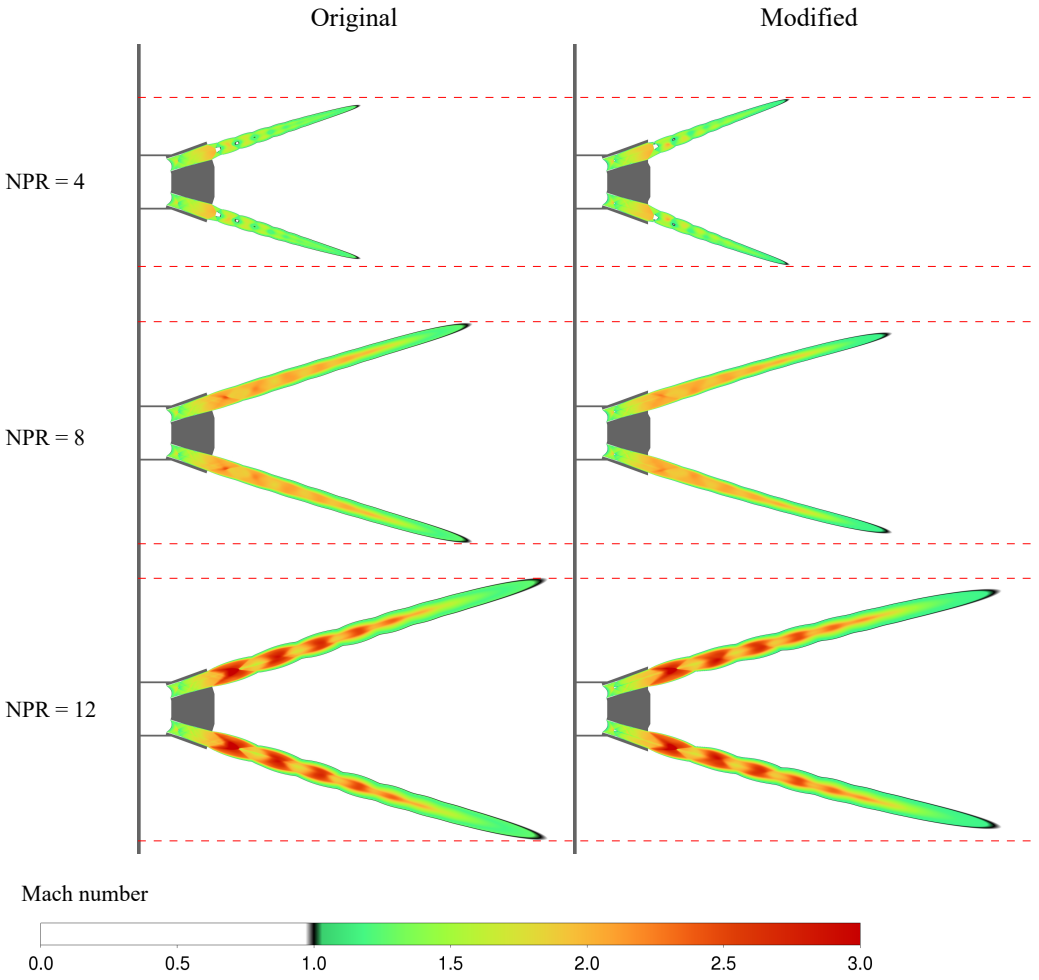

Figure 6. Supersonic core for original and modified configurations at different NPR values.

For the NPR = 8 cases (second row), the supersonic jets are close to the ideal condition, i.e., an isentropic flow without internal shocks and uniform velocity at the outlet. Although some shock waves can be seen, they are not so strong and in practice the ideal condition cannot be achieved. The coalescence of the jet, stronger in the modified case in relation to the original configuration, is also attributed to the momentum balance, as will be explained in the next paragraph for the NPR = 12 case.

The NPR = 12 cases are shown in the third row of Fig. 6. It is clear from the figures that the jets are underexpanded. Although chock waves also appear in this case, the underexpanded condition is usually used in BOF converter operations, as the expansion after the nozzle exit protects it from thermal wear that may occur if the exit pressure is lower than the ambient pressure (overexpansion). For this NPR case (NPR = 12), widely employed in BOF operations, the jet pattern for the original configuration case (left) is almost symmetrical in relation to the center line of the jet. However, for the modified configuration (right), there is a small asymmetry of the jet, and the red region (high Mach number) just after the nozzle outlet, is larger in the inner part of the jet, indicating larger momentum in this region when compared to the outer region of the original case. The larger velocities in this region (higher momentum) led to a larger coalescence of the jets.

To better visualize the asymmetry of the jet in the modified configuration case, the numerical Schilieren pictures (density gradients) for the NPR = 4 cases are shown in Fig. 7. For the original configuration case (left) the main flow structures for an overexpanded jet are observed and a Mach disk with a slip zone is observed just after the nozzle outlet. For the modified configuration case, the Mach disk also occurs but, since the outside nozzle wall is longer, the compression shocks in the outer boards of the nozzles are moved forward in comparison to the compression shocks in the inner boards and for this reason, the Mach disks are eccentric. In general, jet asymmetry shortens the potential core and accelerates jet coalescence, but under certain conditions, such as high NPR values, other factors can influence this behavior. It is not easily monitored, so nozzle designers must take care when selecting lance geometry to minimize these effects.

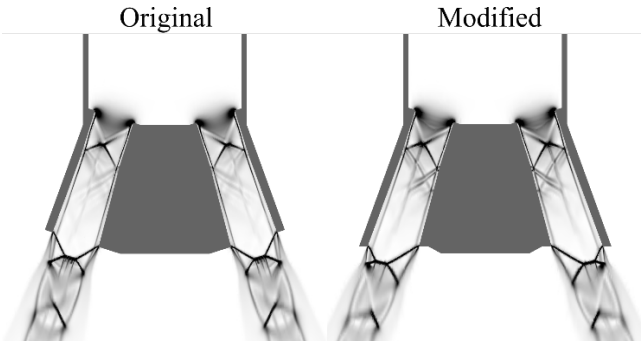

Figure 7. Schlieren images obtained for NPR = 4 at the lance exit.

Figure 8 shows the complete Schilieren pictures for all the cases evaluated in this study. It can be seen in the figure that the potential core increases as the NPR value increases and the modification proposed affects the coalescence of the jets. To better understand the NPR and geometry effects on the coalescence of the jets, Fig. 9 shows path lines of particles that were initially at the center of the nozzle outlet. For the original configuration, at the same axial position, the higher the NPR the bigger the diameter of the jet, as it would be expected. For the modified configuration case, this tendency is also observed for the higher values of NPR (NPR = 8 and 12). However, for the NPR = 4 case, the jet presents a larger diameter, for a given axial position, when compared to the higher NPR cases. This occurrence is due to the asymmetry of the jets that affect the momentum balance and pressure differences between the inner and outer side of the jets.

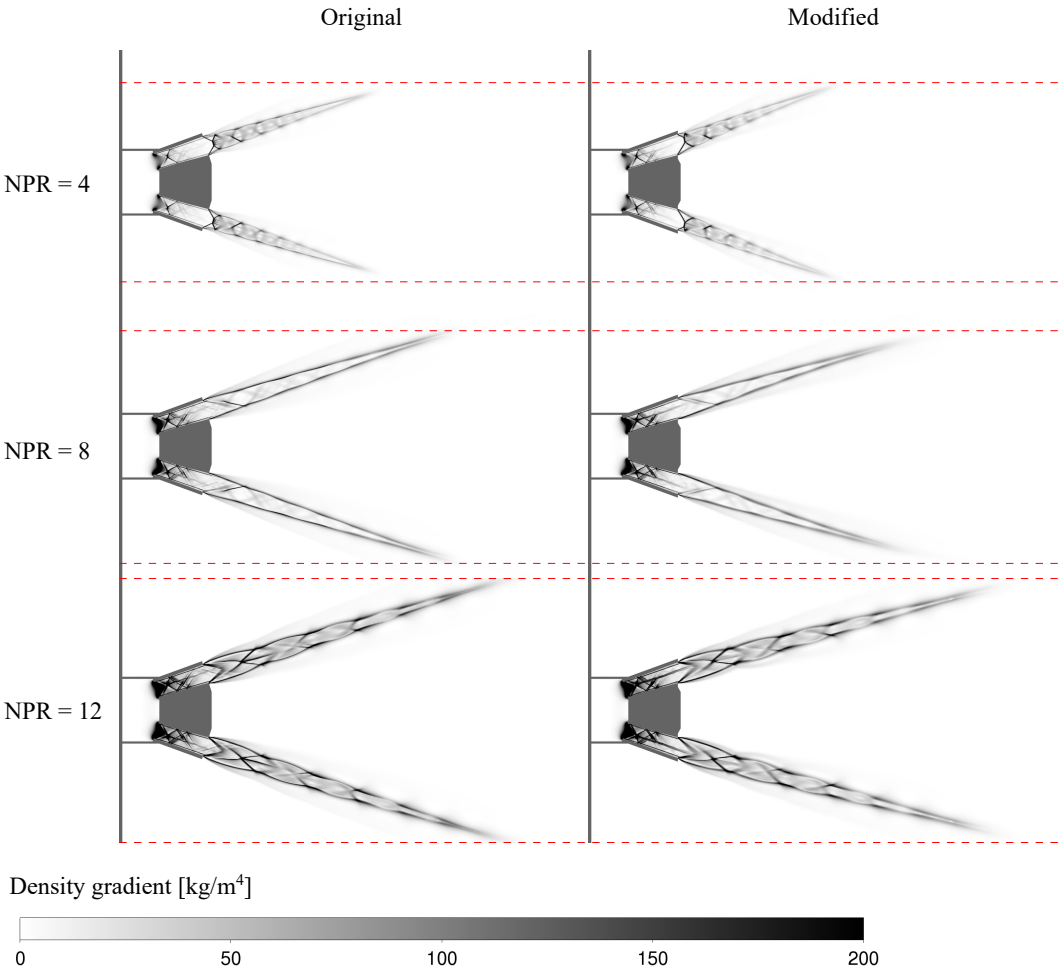

Figure 8. Comparison between the Schlieren images for original and modified configurations at different NPR values.

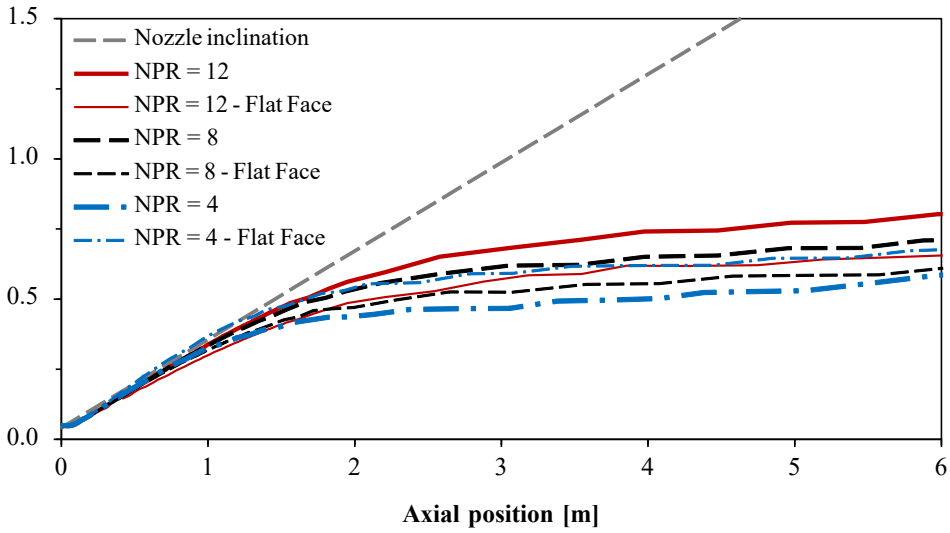

Figure 9. Influence of geometry configuration and NPR value on coalescence of the supersonic jet.

Concerning the supersonic jet length, Fig. 10 show the supersonic core length for different NPR values and both geometries. For NPR = 4 and 8, the original configuration is more appropriate, since it leads to higher values of supersonic core length. However, the NPR = 12 is more usual for BOF operation and, for this pressure ratio, the modified configuration leads to better results, i.e., higher value of supersonic core length (4.6% of increase), which means more mixing for a given lance height.

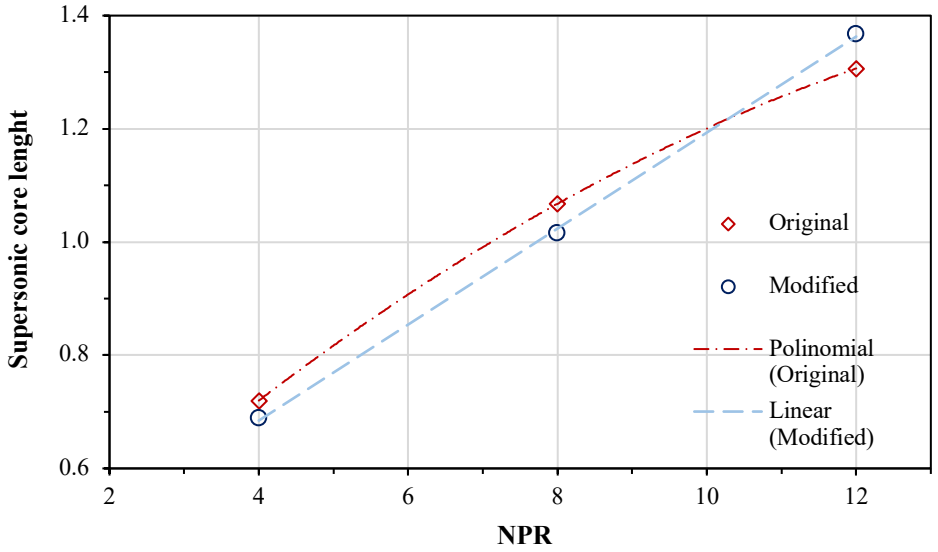

Figure 10. Influence of the Nozzle Pressure Ratio (NPR) on supersonic core length.

Figure 11 compares the vector fields for the original (inclined-face) and modified (flat-face) lance tips at NPR = 4. In the original configuration, the over-expanded jets form shear layers that merge along the center-line and roll up into a paired, co-rotating vortex attached to the inclined surface. Because the local shear is weak, two low-velocity pockets appear, one at the geometric center of the face and another on the sloped section, creating stagnation zones where slag or metal can accumulate. In the modified tip, the flat exit plane diminishes shear-layer interaction; the near-wall vortices reverse sense and are quickly re-entrained by the jets, eliminating the stagnation pockets and thereby reducing the likelihood of material build-up on the lance face.

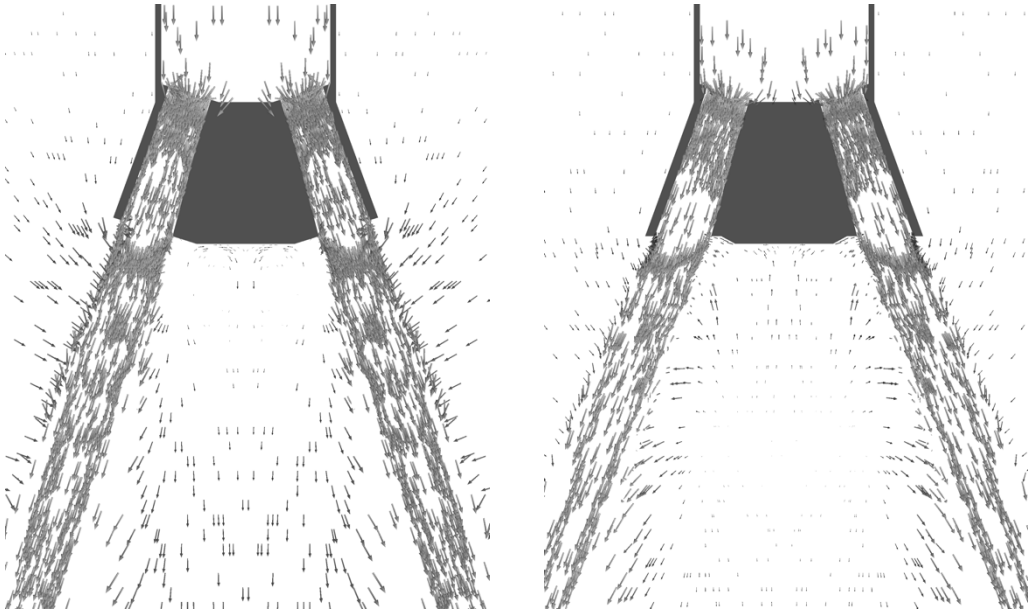

(a) Original (b) Modified

Figure 11. Velocity-vector fields at NPR = 4 for (a) the original inclined-face lance tip and (b) the modified flat-face tip.

Figure 12 compares the velocity-vector fields at NPR = 8 for the original inclined-face and the modified flat-face lance tips. At this higher pressure ratio, the jets issue with greater momentum, but in the original geometry their shear layers interact only weakly; the flow detaches from the inclined surface, creating an extensive, nearly quiescent pocket that blankets both the geometric center and the lower portion of the slope, prime sites for slag or metal deposition. In the modified tip the flat exit plane intercepts the jets more directly, generating a thin, uniform shear layer that slides over the face; although local velocities are modest, the available shear is sufficient to sweep the surface continuously, so no persistent stagnation zone develops and the tendency for material build-up is effectively suppressed.

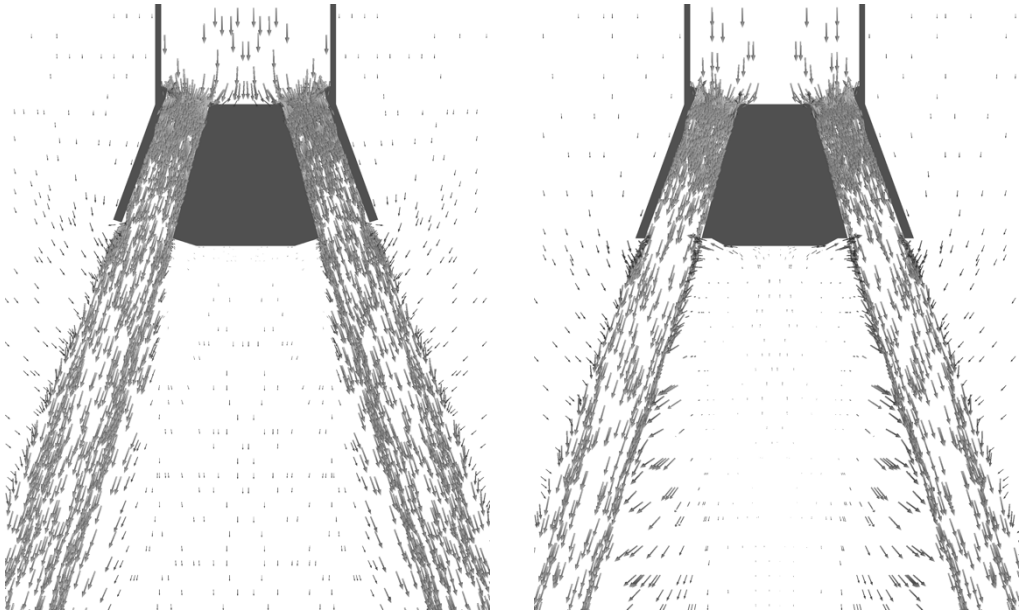

(a) Original (b) Modified

Figure 12. Velocity-vector fields at NPR = 8 for (a) the original inclined-face lance tip and (b) the modified flat-face tip.

Figure 13 compares the vector fields for the original (inclined-face) and modified (flat-face) lance tips at NPR = 12. At this pressure ratio the jets are under-expanded and the interaction between their shear layers strengthens. In the inclined-face tip the converging layers roll up into a complex, multi-cell recirculation; a paired vortex system clings to the wall and drives a downward flow at the center of the face, creating a low-velocity pocket where slag or metal can settle and solidify. In the flat-face tip the jets strike the face nearly normal, the recirculation collapses, and no stagnation zone develops; the price, however, is a higher near-wall velocity and shear that can hasten face wear over long campaigns.

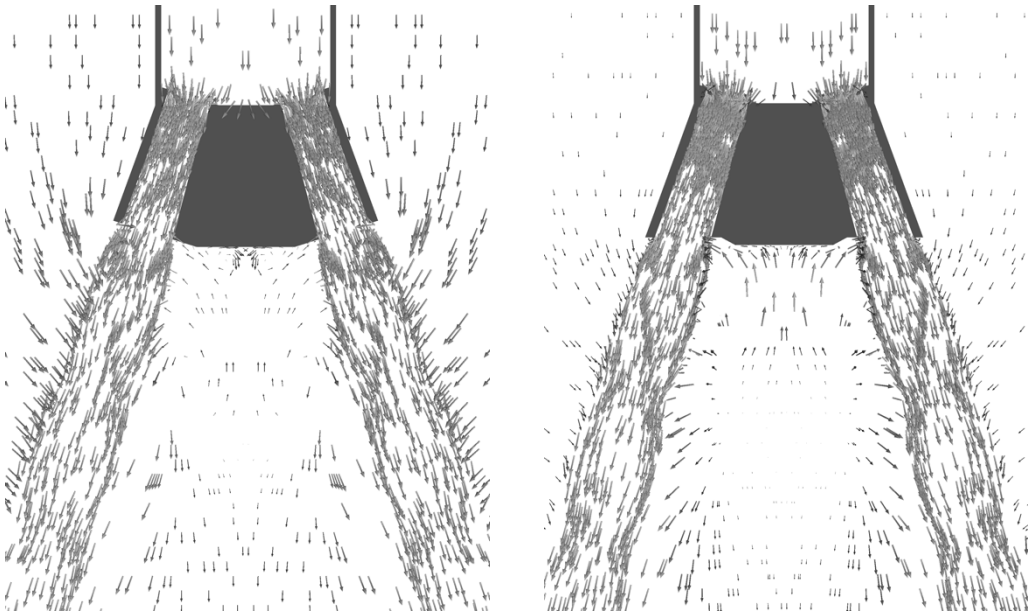

(a) Original (b) Modified

Figure 13. Velocity-vector fields at NPR = 8 for (a) the original inclined-face lance tip and (b) the modified flat-face tip.

CONCLUSIONS

Three-dimensional CFD analyses were carried out to evaluate a simple geometric modification, replacing the conventional inclined lance face with a flat, horizontal exit plane, at three NPR values. At NPR = 4 (over-expanded jets) the flat face inverted the near-wall vortex pair and swept away the low-velocity pockets that normally trap slag or metal. At NPR = 8 (near-ideal expansion) shear-layer interactions were weak for both configurations, but a continuous wall shear was observed in the flat-face configuration, sufficient to avoid metal build-up on the lance face. At NPR = 12 (under-expanded jets) the redesign again removed stagnation zones, virtually eliminating the risk of deposit build-up, although the higher wall-shear levels could cause lance-tip wear if campaigns are prolonged. Overall, the flat-face tip suppresses metal deposition across all operating conditions and should extend lance service intervals, provided that face erosion is routinely monitored at the highest NPR. For future is recommend experimental validation and testing of erosion rates in prolonged campaigns.

ACKNOWLEDGMENTS

This research was funded by the Espírito Santo Research and Innovation Support Foundation (FAPES), Grant No. 1052/2022. The authors gratefully acknowledge this support, which made the present work possible.

REFERENCES

1. M. Li, Q. Li, S. B. Kuang, and Z. Zou. “Coalescence characteristics of supersonic jets from multi-nozzle oxygen lance in *steelmaking bof. steel research international”*, 86(12):1517–1529, 2015. doi: https://doi.org/ 10.1002/srin.201400506.
2. M. M. Li, Q. Li, L. Li, Y. B. He, and Z. S. Zou. “Effect of operation parameters on supersonic jet behaviour of bof six-nozzle oxygen lance”. Ironmaking & Steelmaking, 41(9):699–709, 2014. doi: 10.1179/1743281213Y. 0000000154.
3. C. Feng, R. Zhu, K. Dong, Wei G., B. Han, W. Li, and W. Wu. “Effects of nozzle layout and parameters on the jet characteristics of a CO_2 + O_2 mixed oxygen lance”. Metall Mater Trans B, 52(12):425–439, 2021. doi: https://doi.org/10.1007/s11663-020-02048-8.
4. P. F. Garcia, Zotelle A. C., R. N. Siqueira, J. P. Barbosa, B. T. Maia, and J. R. Oliveira. “Numerical analysis of the effects of convergent-divergent nozzle geometry on the characteristics of supersonic jet in bof converters”. In COBEM 2023, pages 1–10. Proceedings of the 27th International Congress of Mechanical Engineering, 2023.
5. M. Alam, J. Naser, and G. Brooks. “Computational fluid dynamics simulation of supersonic oxygen jet behavior at steelmaking temperature”. Metall Mater Trans B, 41:636–645, 2010. doi: https://doi.org/10. 1007/s11663-010-9341-0.
6. W. Wang, Z. Yuan, H. Matsuura, H. Zhao, C. Dai, and F. Tsukihashi. “Three-dimensional compressible flow simulation of top-blown multiple jets in converter”. ISIJ International, 50(4):491–500, 2010. doi: 10.2355/ isijinternational.50.491.
7. X. Zhou, M. Ersson, L. Zhong, J. Yu, and P. Jönsson. “Mathematical and physical simulation of a top blown converter”. steel research international, 85(2):273–281, 2014. doi: hhttps://doi.org/10.1002/srin.201300310.
8. B. T. Maia, R. K. Imagawa, A. C. Petrucelli, and R. P. Tavares. “Effect of blow parameters in the jet penetration by physical model of bof converter”. Journal of Materials Research and Technology, 3(3):244– 256, 2014. ISSN 2238-7854. doi: https://doi.org/10.1016/j.jmrt.2014.06.010.
9. B. T. Maia, A. R. Ribeiro, B. O. Santos, C. A. Souza, F. S. Garajau, and M. Guerra. “Continuous developments at the steel plant 1 usiminas ipatinga through slagless technology”. AISTech - Iron and Steel Technology Conference Proceedings, 2:2125–2135, 01 2015.
10. R. Sambasivam, S. N. Lenka, F. Durst, M. Bock, S. Chandra, and S. K. Ajmani. “A new lance design for bof steelmaking”. Metall Mater Trans B, 38:45–53, 2007. doi: https://doi.org/10.1007/s11663-006-9004-3.
11. Y. Higuchi and Y. Tago. “Effect of nozzle twisted lance on jet behavior and spitting rate in top blown process”. ISIJ International, 43(9):1410–1414, 2003. doi: 10.2355/isijinternational.43.1410.
12. F. S. Garajau, M. S. L. Guerra, B. T. Maia, P. R. Cetlin, and D. A. Moreira. Case study: “Wear in supersonic nozzle of tip lance in vallourec brazil steelmaking”. In AISTech 2017, volume 1, pages 1365–1375. Proceedings of the Iron & Steel Technology Conference. Warrendale: Association for Iron & Steel Technology, 2017.
13. A. Hadjadj, Y. Perrot, and S. Verma. “Numerical study of shock/boundary layer interaction in supersonic overexpanded nozzles”. Aerospace Science and Technology, 42:158–168, April 2015. ISSN 1270-9638. doi: 10.1016/j.ast.2015.01.010.
14. A. Yaravintelimath, B.N. Raghunandan, and J. Moríñigo. “Numerical prediction of nozzle flow separation: Issue of turbulence modeling”. Aerospace Science and Technology, 50:31–43, March 2016. ISSN 1270-9638. doi: 10.1016/j.ast.2015.12.016.
15. F. R. Menter. “Two-equation eddy-viscosity turbulence models for engineering applications”. AIAA Journal, 32(8):1598 – 1605, 1994.
16. Ansys INC. “Ansys Fluent Theory Guide”. ANSYS Inc, Canonsburg, PA, release 2021 r2 edition, 2021.
17. B. T. Maia, W. R. Lima, and R. R. Nascimento. “Analysis of geometrical aspects of bof converters and correlations with process parameters”. In European Steel Technology and Applications Days 2017. ESTAD 2017, July 2017.
18. O. Igra, L. Wang, J. Falcovitz, and O. Amann. “Simulation of the starting flow in a wedge-like nozzle”. Shock Waves, 8(4):235–242, August 1998. ISSN 1432-2153. doi: 10.1007/s001930050116.
19. A. S. Mouronval and A. Hadjadj. “Numerical study of the starting process in a supersonic nozzle”. Journal of Propulsion and Power, 21(2):374–378, March 2005. ISSN 1533-3876. doi: 10.2514/1.6122.
20. P. V. Raje and K. Sinha. “Three-dimensional simulation of rocket nozzles with multi-jet interaction using shock-unsteadiness model”. In Proceedings of the AIAA Aviation Forum, pages 1–15, Dallas, Texas, 2019.

21. V. I. Zapryagaev, A. N. Kudryavtsev, A. V. Lokotko, A. V. Solotchin, and A. Hadjadj. “An experimental and numerical study of a supersonic-jet shock-wave structure”. In West East High Speed Flow Fields. edited by D. E. Zeitoun et al. (CIMNE, Barcelona, 2003), July 2002.